Precision & Performance Conference 2025, Cranfield University, UK, 17th- 20th November 2025

Dual-Method Design Exploration for Parametric Sensitivity and Performance Optimization in CF-PA6 Additive Manufacturing

A. Abdullah[1*], A. Iqbal[1], M. Ayaz[1], T. A. Shams[1], Naeem. S. Mian[2]

[1]*College of Aeronautical Engineering, National University of Sciences and Technology (NUST), H-12, Islamabad, Pakistan*

[2]*Centre for Precision Technologies, School of Computing and Engineering, University of Huddersfield, Queensgate, Huddersfield HD1 3DH, UK*

aabdullah.im01cae@student.nust.edu.pk

Abstract

Material characteristics play a significant role in the engineering design process. Enhancing these properties through improved processing techniques and tighter process control is essential for achieving optimal outcomes. Fiber-reinforced additive manufacturing (FRAM) enables the production of composite parts with high mechanical performance, with Fused Filament Fabrication (FFF) being the most common AM method using fibre-reinforced polymer filaments. Among these, carbon fibre reinforced polyamide (CF-PA) is of particular interest due to its favourable strength-to-weight ratio and thermal stability.

The properties of short carbon fibre reinforced polyamide composites are highly sensitive to variations in process parameters. In this study, a dual-phase experimental strategy was employed to investigate the influence of key FFF process parameters on the performance of carbon fibre reinforced polyamide (CF-PA6) parts. Five control factors, print temperature (260, 265, 270, 275 °C), print speed (10, 20, 30, 40 mm/s), layer height (0.1, 0.18, 0.26, 0.35 mm), raster angle (0°, 30°, 60°, 90°), and infill percentage (70%, 80%, 90%, 100%) were examined using a structured Taguchi L16 orthogonal array to assess the main effects of each parameter. To complement this design and explore the intermediate design space between the individual factor levels more thoroughly, Latin Hypercube Sampling (LHS) was employed with additional 18 runs.

The comparative evaluation of Taguchi L16 and LHS results in this research enabled the extraction of both general trends and localized sensitivities across the focused parameter ranges. While the Taguchi method provides a highly efficient framework for identifying influential parameters and optimizing within defined levels, the LHS design offers finer resolution and captures variations within the gaps left by orthogonal designs. By analyzing both datasets for porosity and print time, this approach allows for a better understanding of parameter scalability, helps identify stable processing windows, and supports more informed decision-making in fiber-reinforced additive manufacturing. This integrated methodology thus strengthens process insight by balancing statistical efficiency with design space exploration.

Fused Filament Fabrication, Design of Experiments, Taguchi, Latin Hypercube, Porosity, Print Time

1. Introduction

Fused Filament Fabrication (FFF) has emerged as a widely adopted additive manufacturing (AM) method, offering the capability to produce complex geometries with cost-effectiveness and rapid turnaround [1][2][3]. The quality and performance of parts are dependent on various process parameters suh as nozzle temperature, print speed, layer height, and raster angle [4], [5], [6]. Process parameters critically influence the fundamental aspects of the printing process, such as bead deposition and inter-layer fusion which profoundly impact the final properties of the printed components. Among the various materials utilized in FFF, carbon fiber reinforced polyamide (CF-PA) has garnered significant attention, particularly for high-performance applications. Its appeal stems from a favorable strength-to-weight ratio and commendable thermal stability [2], [7], [8]. However, despite these advantages, CF-PA parts are prone to defects, including dimensional inaccuracies and porosity, which can compromise both their mechanical performance and geometric fidelity [9]. Such sensitivities require robust and effective process control strategies to ensure consistent and high-quality production.

Traditional Design of Experiments (DoE) methodologies, such as full factorial designs and Taguchi methods, have historically proven valuable for initial parameter screening and identifying robust factors in manufacturing processes [1], [10]. Nevertheless, the conventional Taguchi approach, while efficient for initial assessments, possesses inherent limitations, particularly its single-level evaluation which often fails to adequately capture higher-order interactions among process parameters [11], [12], [13]. To address this critical gap and achieve a more comprehensive understanding of the complex interplay between parameters and material properties, this study employs a dual-method experimental strategy. This approach integrates the structured efficiency of a Taguchi L16 orthogonal array with the detailed design space exploration offered by Latin Hypercube Sampling (LHS) [14].

The primary objective of this research is to investigate the influence of key FFF process parameters on the performance of CF-PA6 parts, specifically focusing on porosity and print time. By combining Taguchi L16 (for assessing main effects and general trends) with LHS (for exploring intermediate design spaces and localized sensitivities), this integrated methodology aims to provide a deeper insight into parameter scalability, identify stable processing windows, and ultimately support more

informed decision-making in fiber-reinforced additive manufacturing. This balanced approach seeks to enhance process insight by synergistically leveraging statistical efficiency with comprehensive design space exploration, paving the way for more robust and predictable manufacturing outcomes.

2. Methodology

2.1. Materials and Equipment

For this study, short carbon fiber reinforced PA6 (CF-PA6) filament with a diameter of 1.75 mm was utilized. Printing was conducted on an IEMAI Magic HT Pro high-temperature FFF printer, which features an enclosed chamber to maintain a controlled thermal environment. A 0.4 mm hardened nozzle was employed for material extrusion. Throughout the printing process, the chamber temperature was consistently maintained at 110 °C, and the bed temperature at 120 °C. Cooling fans were deliberately kept off to prevent premature cooling and ensure optimal inter-layer adhesion. All samples were printed in a constant orientation to ensure consistency. The geometry of the specimens adhered to the ASTM D6110 (**Standard Test Method for Determining the Charpy Impact Resistance of Notched Specimens of Plastics)** standard for rectangular impact test samples, measuring 124.5 × 12.7 × 7.85 mm.

Figure 1: IEMAI magic HT Pro Printer; ASTM D6110 samples

2.2. Experimental Design and Measurements

To systematically investigate the influence of key FFF process parameters, a dual-phase experimental design was implemented. The initial phase involved a structured Taguchi L16 orthogonal array, which allowed for the efficient assessment of main effects from five control factors, each examined at four distinct levels. These factors included print temperature (260, 265, 270, 275 °C), print speed (10, 20, 30, 40 mm/s), layer height (0.1, 0.18, 0.26, 0.35 mm), raster angle (0°, 30°, 60°, 90°), and infill percentage (70%, 80%, 90%, 100%). This Taguchi design provided a robust framework for identifying the most influential parameters and establishing general trends within the defined experimental range.

Table 1: L16 Dataset

Run	Prin Temp (°C)	Print Speed (mm/s)	Laye Height (mm)	Raster Angle(°)	Infill Density (%)	Prin Time (min)	Porosity(%)
1	260	10	0.1	0	70	612	4.724
2	260	20	0.18	30	80	247	6.795
3	260	30	0.26	60	90	150	6.657
4	260	40	0.35	90	100	103	7.434
5	265	10	0.18	60	100	469	2.790
6	265	20	0.1	90	90	409	4.036
7	265	30	0.35	0	80	120	9.144
8	265	40	0.26	30	70	118	10.023
9	270	10	0.26	90	80	359	6.087
10	270	20	0.35	60	70	158	13.038
11	270	30	0.1	30	100	326	6.190
12	270	40	0.18	0	90	165	2.515
13	275	10	0.35	30	90	301	9.616
14	275	20	0.26	0	100	209	5.064
15	275	30	0.18	90	70	186	12.605
16	275	40	0.1	60	80	254	7.746

Complementing the Taguchi L16 array, a second phase of experimentation utilized Latin Hypercube Sampling (LHS). An additional 18 runs were generated using LHS to thoroughly explore the intermediate design space that might be left uncovered by the discrete levels of the orthogonal array. This approach provided a different perspective of the parameter landscape, allowing for the capture of localized sensitivities and variations that might otherwise be missed by Taguchi analysis. For both experimental sets, the primary performance metrics measured were porosity and print time. Porosity was quantified to assess the internal quality and density of the printed parts, while print time was recorded to evaluate the manufacturing efficiency across different parameter combinations. Crucially, the data from the Taguchi L16 array and the Latin Hypercube Sampling runs will be treated as distinct datasets for subsequent analysis. The comparative analysis of these two datasets aimed to provide a comprehensive understanding of parameter scalability, identify stable processing windows, and support more informed decision-making in fiber-reinforced additive manufacturing.

Table 2: LHS18 Dataset

Run	Print Temp (°C)	Print Speed (mm/s)	Layer Height (mm)	Raster Angle(°)	Infill Density (%)	Print Time (min)	Porosity(%)
1	261	37	0.28	66	77	119	12.077
2	268	25	0.35	18	98	144	5.929
3	267	13	0.1	48	87	553	4.248
4	272	39	0.27	63	79	119	10.689
5	262	37	0.29	84	77	117	11.308
6	271	36	0.28	6	97	129	11.121
7	265	27	0.22	72	98	184	7.729
8	265	16	0.24	44	99	261	9.418
9	266	38	0.14	33	75	196	7.943
10	270	23	0.11	25	76	320	6.236
11	261	30	0.31	43	83	131	11.370
12	260	29	0.3	59	74	133	7.988
13	271	25	0.17	10	71	214	6.409
14	269	16	0.34	51	90	204	6.979
15	275	26	0.16	2	96	240	8.550
16	270	28	0.19	76	96	200	6.249
17	275	40	0.26	90	70	79	6.864
18	275	40	0.35	30	80	65	4.689

3. Results and Discussion

3.1. Data Preprocessing

The LHS dataset was subjected to an outlier detection procedure using the interquartile range (IQR) method. One

anomalous data point (Experiment No. 3) was identified and removed prior to statistical analysis, reducing the dataset to 17 valid runs. This step ensured the robustness of subsequent ANOVA and trend evaluations, consistent with recommended practices in DoE-based additive manufacturing studies [15].

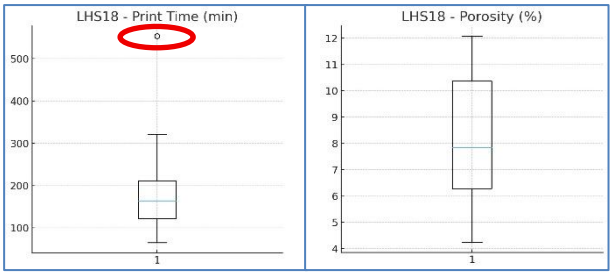

Figure 2: Box plots of Print Time and Porosity (LHS18 dataset), depicting outlier in print time readings

3.2. Taguchi L16 Analysis

ANOVA results for the Taguchi dataset (Table 3) revealed that **print speed (50.7%)** and **layer height (35.5%)** were the dominant contributors to **print time**, jointly accounting for over 86% of the observed variance. Print temperature, raster angle, and infill density contributed negligibly (<2% each). The trend aligns with physical expectations, as higher speeds and larger layer heights directly reduce deposition time per unit volume. Similar dominance of these two factors has been widely reported in FFF process optimization across both neat polymers and fiber-reinforced composites [16].

For **porosity** (Table 4), **infill density (34.7%)** and **layer height (24.4%)** emerged as the most influential parameters, followed by print temperature (7.8%). Scatter plots (Figure 3) confirmed these findings: porosity decreased consistently at higher infill densities and lower layer heights, consistent with improved interlayer packing and reduced void formation. These results are in line with prior studies showing that geometric deposition control, particularly infill strategy, plays a dominant role in porosity minimization in fiber-reinforced PA6 and similar composites [17].

Table 3: ANOVA results of Print Time (L16)

	sum_sq	df	F	PR(>F)	Factor Contributions (%)
Print_Temp	4410.45	1	1.161053	0.306554	1.423618
Print_Speed	156999.2	1	41.33013	7.55E-05	50.676658
Layer_Height	110004.476	1	28.95874	0.00031	35.507564
Raster_Angle	145.8	1	0.038382	0.848602	0.047062
Infill_Density	259.2	1	0.068235	0.799226	0.083665
Residual	37986.6241	10			12.261433

Table 4: ANOVA results of Porosity (L16)

	sum_sq	df	F	PR(>F)	Factor Contributions (%)
Print_Temp	11.324	1	3.080566	0.109762	7.755239
Print_Speed	4.592413	1	1.249314	0.289816	3.145114
Layer_Height	35.59279	1	9.68262	0.011029	24.375725
Raster_Angle	7.052266	1	1.91849	0.196141	4.829744
Infill_Density	50.69644	1	13.7914	0.004017	34.719459
Residual	36.75947	10			25.17472

3.3. Latin Hypercube Sampling (LHS) Analysis

The LHS dataset provided finer resolution across the design space. For **print time** (Table 5), the dominant contributors were again **layer height (51.5%)** and **print speed (39.6%)**, together explaining over 91% of variance. Other factors contributed <1% each, reaffirming the Taguchi trends. This close agreement with Taguchi validates that deposition rate is fundamentally controlled by geometric scaling, as reported in earlier parametric studies [18].

In contrast, **porosity** (Table 6) **behavior differed notably**. Here, **print temperature (28.9%)** emerged as the most significant factor, followed by print speed (15.0%). Infill density contributed modestly (5.0%), while layer height and raster angle were negligible (<1%). Results indicated that porosity decreased at higher extrusion temperatures, suggesting enhanced polymer diffusion and fiber–matrix bonding. This agrees with prior investigations that identified thermal processing as critical for void reduction in short- and continuous-fiber thermoplastic composites [19].

Table 5: ANOVA results of Print Time (LHS18)

	sum_sq	df	F	PR(>F)	Factor Contributions (%)
Print_Temp	118.7277	1	0.358766	0.561325	0.251373
Print_Speed	18710.06	1	56.53719	1.17E-05	39.613414
Layer_Height	24342.56	1	73.55723	3.35E-06	51.538692
Raster_Angle	403.0647	1	1.217962	0.293319	0.853379
Infill_Density	16.9417	1	0.051194	0.825148	0.035869
Residual	3640.271	11			7.707273

Table 6: ANOVA results of Porosity (LHS18)

	sum_sq	df	F	PR(>F)	Factor Contributions (%)
Print_Temp	26.71425	1	6.315494	0.028829	28.895976
Print_Speed	13.84731	1	3.27363	0.097783	14.978202
Layer_Height	0.308887	1	0.073024	0.791987	0.334113
Raster_Angle	0.431203	1	0.10194	0.755495	0.466419
Infill_Density	4.618586	1	1.091876	0.318475	4.99578
Residual	46.5295	11			50.329511

3.3. Comparative Insights

Both experimental strategies consistently identified **layer height and print speed as the primary drivers of print time**, underscoring their critical role in production efficiency. For porosity, however, the two methods highlighted different sensitivities. While Taguchi emphasized **geometric parameters (layer height, infill density)**, LHS revealed a stronger dependence on **thermal control (print temperature)**. This divergence underscores the value of combining orthogonal and space-filling designs: Taguchi efficiently captures robust main effects, while LHS uncovers localized or nonlinear trends between factor levels.

Mechanistically, higher infill and lower layer height reduce void formation through increased overlap between deposition roads [17]. Conversely, elevated extrusion temperature enhances interlayer diffusion and fiber–matrix adhesion, explaining the temperature sensitivity revealed in LHS but muted in Taguchi [19]. These combined effects illustrate a trade-off: minimizing porosity requires careful balancing of both **geometric deposition parameters** and **thermal processing conditions**.

3.3. Processing Windows and Implications

The dual-method approach demonstrates that **robustly low print times** can be achieved through high print speeds and large layer heights, albeit with a penalty in porosity. Conversely,

minimizing porosity favors high infill density, reduced layer heights, and higher extrusion temperatures. These results suggest a **stable process window** where efficiency and part quality can be jointly optimized by maintaining moderate layer heights (≈0.18–0.26 mm), high infill (>90%), and elevated nozzle temperatures (≥270 °C), while adjusting print speed according to the acceptable porosity–time trade-off.

By integrating Taguchi and LHS methodologies, this study establishes a more comprehensive understanding of parameter scalability and sensitivities in CF-PA6 FFF. The findings highlight the importance of complementing efficient orthogonal designs with space-filling sampling to capture both broad trends and fine-scale effects, thereby enabling more reliable process optimization in fiber-reinforced additive manufacturing.

4. Conclusion

This study investigated the influence of five key FFF parameters on the porosity and print time of short carbon fiber–reinforced PA6 using a dual-phase experimental approach. Taguchi L16 efficiently identified dominant factors, with print speed and layer height accounting for over 85% of the variance in print time, and infill density and layer height governing porosity. Complementary analysis with Latin Hypercube Sampling revealed additional sensitivities, particularly the significant effect of extrusion temperature on porosity, which was not captured in the orthogonal design.

The integrated Taguchi–LHS methodology thus provided both broad trends and fine-scale insights, enabling the identification of stable processing windows where part quality and production efficiency can be jointly optimized. These findings highlight the importance of combining structured and space-filling experimental strategies for process characterization in fiber-reinforced additive manufacturing.

5. Future Work

Future efforts will extend this dual-method approach to include **mechanical performance metrics** such as impact strength and interlaminar shear strength, providing a direct link between processing parameters, porosity, and structural properties. Additionally, the experimental datasets will serve as training input for **machine learning models**, particularly Gaussian Process Regression with Automatic Relevance Determination (GPR-ARD), to predict and optimize parameter combinations beyond the tested ranges.

Further studies will also explore **multi-objective optimization frameworks** to balance porosity reduction, mechanical performance, and manufacturing efficiency. Finally, microstructural characterization (e.g., X-ray CT, SEM) will be incorporated to provide deeper insights into void morphology and fiber–matrix interactions under varying process conditions.

References

[1] J. Wong, A. Altassan, and D. W. Rosen, “Additive manufacturing of fiber-reinforced polymer composites: A technical review and status of design methodologies,” *Compos. Part B Eng.*, vol. 255, p. 110603, Apr. 2023, doi: 10.1016/j.compositesb.2023.110603.

[2] B. Brenken, E. Barocio, A. Favaloro, V. Kunc, and R. B. Pipes, “Fused filament fabrication of fiber-reinforced polymers: A review,” *Addit. Manuf.*, vol. 21, pp. 1–16, May 2018, doi: 10.1016/j.addma.2018.01.002.

[3] Q. Song *et al.*, “Research on Void Dynamics during In Situ Consolidation of CF/High-Performance Thermoplastic Composite,” *Polymers (Basel).*, vol. 14, no. 7, p. 1401, Mar. 2022, doi: 10.3390/polym14071401.

[4] A. Pulipaka, K. Gide, A. Beheshti, and Z. Bagheri, “Effect of 3D printing process parameters on surface and mechanical properties of FFF-printed PEEK,” *J. Manuf. Process.*, 2023, doi: 10.1016/j.jmapro.2022.11.057.

[5] K. M. Agarwal, P. Shubham, D. Bhatia, P. Sharma, H. Vaid, and R. Vajpeyi, “Analyzing the Impact of Print Parameters on Dimensional Variation of ABS specimens printed using Fused Deposition Modelling (FDM),” *Sensors Int.*, vol. 3, p. 100149, 2022, doi: 10.1016/j.sintl.2021.100149.

[6] S. Srinivasan Ganesh Iyer and O. Keles, “Effect of raster angle on mechanical properties of 3D printed short carbon fiber reinforced acrylonitrile butadiene styrene,” *Compos. Commun.*, vol. 32, p. 101163, Jun. 2022, doi: 10.1016/j.coco.2022.101163.

[7] K. Rithika and J. Sudha, “Additive Manufacturing of Fiber-Reinforced Composites—A Comprehensive Overview,” Dec. 01, 2024, *John Wiley and Sons Ltd*. doi: 10.1002/pat.70002.

[8] N. van de Werken, H. Tekinalp, P. Khanbolouki, S. Ozcan, A. Williams, and M. Tehrani, “Additively manufactured carbon fiber-reinforced composites: State of the art and perspective,” Jan. 01, 2020, *Elsevier B.V.* doi: 10.1016/j.addma.2019.100962.

[9] S. Wickramasinghe, T. Do, and P. Tran, “FDM-Based 3D Printing of Polymer and Associated Composite: A Review on Mechanical Properties, Defects and Treatments,” *Polymers (Basel).*, vol. 12, no. 7, p. 1529, Jul. 2020, doi: 10.3390/polym12071529.

[10] S. Chen, L. Cai, Y. Duan, X. Jing, C. Zhang, and F. Xie, “Performance enhancement of <scp>3D</scp> -printed carbon fiber-reinforced nylon 6 composites,” *Polym. Compos.*, vol. 45, no. 6, pp. 5754–5772, Apr. 2024, doi: 10.1002/pc.28161.

[11] B. Beylergil, A. Al-Nadhari, and M. Yildiz, “Optimization of Charpy-impact strength of <scp>3D</scp> -printed carbon fiber/polyamide composites by Taguchi method,” *Polym. Compos.*, vol. 44, no. 5, pp. 2846–2859, May 2023, doi: 10.1002/pc.27285.

[12] G. Taguchi, *Introduction to quality engineering: designing quality into products and processes*. 1986.

[13] K. Stergiou, C. Ntakolia, P. Varytis, E. Koumoulos, P. Karlsson, and S. Moustakidis, “Enhancing property prediction and process optimization in building materials through machine learning: A review,” *Comput. Mater. Sci.*, vol. 220, p. 112031, Mar. 2023, doi: 10.1016/j.commatsci.2023.112031.

[14] M. D. Shields and J. Zhang, “The generalization of Latin hypercube sampling,” *Reliab. Eng. Syst. Saf.*, vol. 148, pp. 96–108, Apr. 2016, doi: 10.1016/j.ress.2015.12.002.

[15] C. S. K. Dash, A. Behera, S. Dehuri, and A. Ghosh, “An outliers detection and elimination framework in classification task of data mining,” *Decis. Anal. J.*, 2023, doi: 10.1016/j.dajour.2023.100164.

[16] A. Jain, K. Kant, S. Singh, A. Sahai, and R. Sharma, “Process parameter tailored evaluation of FFF-fabricated carbon fibre based poly-lactic-acid composites,” *J. Thermoplast. Compos. Mater.*, vol. 36, pp. 4365–4387, 2023, doi: 10.1177/08927057231155858.

[17] R. Zhang, L. Yu, K. Chen, P. Xue, M. Jia, and Z. Hua, “Amelioration of interfacial properties for CGF/PA6 composites fabricated by ultrasound-assisted FDM 3D printing,” *Compos. Commun.*, vol. 39, p. 101551, Apr. 2023, doi: 10.1016/j.coco.2023.101551.

[18] C.-C. Tseng, Y.-C. Wang, and M.-I. Ho, “Scaling laws and numerical modelling of the laser direct energy deposition,” *Int. J. Heat Mass Transf.*, 2023, doi: 10.1016/j.ijheatmasstransfer.2023.124717.

[19] D. Saenz-Castillo, M. Martín, S. Calvo, F. Rodriguez-Lence, and A. Güemes, “Effect of processing parameters and void content on mechanical properties and NDI of thermoplastic composites,” *Compos. Part A Appl. Sci. Manuf.*, 2019, doi: 10.1016/J.COMPOSITESA.2019.03.035.